2014 American Control Conference (ACC)
June 4-6, 2014. Portland, Oregon, USA

Study of wheel slip and traction forces in differential drive robots and slip avoidance control strategy*

Edison Orlando Cobos Torres, Shyamprasad Konduri, and Prabhakar R. Pagilla[1]

Abstract— **The effect of wheel slip in differential drive robots is investigated in this paper. We consider differential drive robots with two driven wheels and ball-type caster wheels that are used to provide balance and support to the mobile robot. The limiting values of traction forces for slip and no slip conditions are dependent on wheel-ground kinetic and static friction coefficients. The traction forces are used to determine the fraction of input torque that provides robot motion and this is used to calculate the actual position of the robot under slip conditions. The traction forces under no slip conditions are used to determine the limiting value of the wheel torque above which the wheel slips. This limiting torque value is used to set a saturation limit for the input torque to avoid slip. Simulations are conducted to evaluate the behavior of the robot during slip and no slip conditions. Experiments are conducted under similar slip and no slip conditions using a custom built differential drive mobile robot with one caster wheel to validate the simulations. Experiments are also conducted with the torque limiting strategy. Results from model simulations and experiments are presented and discussed.**

I. INTRODUCTION

Research related to mobile robots in a variety of areas, such as dynamic modeling, control design, coordination, has been active in the last several decades. Because of their simplicity in construction and dynamics, differential drive mobile robots have been the most common configurations considered. A typical differential drive robot consists of two driven wheels and one or more caster wheels. Most of the research in differential drive robots has assumed pure rolling of robot wheels, that is, all the torque provided to the robot wheels is used to provide motion to the robot. Kinematics and dynamics of these types of mobile robots and controller designs for achieving various motion objectives have been considered in literature [1]–[4]. In practice the pure rolling assumption does not always hold, especially in circumstances where large values of input torque are used to accelerate the wheels, thereby resulting in wheel slip. The inability to reach the desired position due to wheel slip has been reported in the literature; such examples are presented in [5], [6] where wheel slip causes problems in tracking and the inability to maintain desired distance between vehicles in coordination maneuvers.

Wheel slip can occur in the longitudinal and/or lateral direction of the wheel motion. It depends on the wheel accelerations and the traction forces between the wheels and the ground. The interaction between the ground and the wheel could be complex depending on the various types of wheel and ground properties that are considered; for example soft rubber covered wheels, loose soil, etc. There are several theories and approximations to describe these interactions [7]; many studies use the properties of tire and ground to determine the coefficient of friction and traction forces. Although these models provide considerable understanding of slip, they require a number of parameters to characterize the wheel and ground behavior during motion. Methods have been developed for predicting and controlling the behavior of the robot when it slips [8]–[14]. In these studies the kinematics and dynamics under slip conditions are modeled by considering either a flexible wheel, rigid ground or rigid wheel, flexible ground interaction. Some literature in the last decade has focused on rigid wheel, rigid ground interaction [5] and [15]. In [5] a relationship between the traction forces and applied wheel torques is obtained without considering the portion of mass supported by each wheel; a two stage controller is employed for trajectory tracking. It is indicated that the measurement of the global location of the robot is necessary to effectively control the robot. In [15], the traction forces are determined by using the static friction coefficient between the wheel and the ground for both slip and non-slip conditions. In previous studies, the effect of the caster wheel is ignored when calculating the normal forces.

In this work, wheel slip with a rigid wheel, rigid ground interaction is considered, since it best represents the wheel-ground interaction of the robots used as part of this research. The traction forces are determined by

*This work is supported by National Science Foundation under Grant No. 0825937.

[1]E. O. Cobos, S. Konduri and P. R. Pagilla are with the School of Mechanical and Aerospace Engineering, Oklahoma State University, Stillwater, OK 74078, USA pagilla at okstate.edu

using both static and kinetic coefficients of friction unlike the previous studies which use only the static friction coefficient for both slip and non-slip conditions. The linear velocities of the wheel are used in computing the traction forces instead of slip velocities. The effect of caster wheel is also included in calculating the normal forces. A simple slip avoidance control strategy is proposed based on the traction forces. The behavior of the robot is simulated and experimentally verified for both slip and non-slip conditions. The proposed control strategy is also validated through experiments. The rest of this paper is organized as follows. The kinematics and dynamics of the differential drive robot under slip conditions are described in Section II. The traction forces are given in Section III. A simple control strategy to avoid wheel slip is also discussed. Model simulations and sample experimental results are given in Section IV. Finally conclusions of this work are presented in Section V.

II. MOBILE ROBOT DYNAMICS

Consider a sketch of differential drive robot shown in Figure 1.

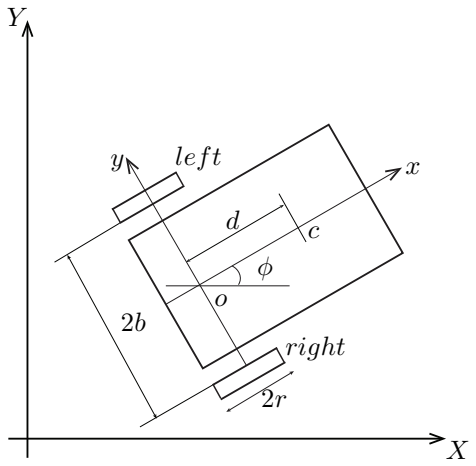

Fig. 1: Two Wheeled Differential Drive Robot

Let the position of the robot be given by the vector $[x_c, y_c, \phi]^T$, where (x_c, y_c) denote the position of point c (the center of mass) and ϕ is the orientation of the robot in the global coordinate frame. The angular velocity of the wheel is denoted by $\dot{\theta}$ and subscripts r and l denote left and right wheel, respectively. The generalized position vector of the robot is $q = [x_c, y_c, \phi, \theta_r, \theta_l]^T$. The control inputs are the wheel torques (τ_r, τ_l). Let $s_\phi = \sin\phi$, $c_\phi = \cos\phi$, b is half of the wheel base, d is the distance between the center of the mass and wheel axis. The kinematics under the pure rolling condition are given by

$$\left.\begin{aligned} \dot{\theta}_r r &= \dot{x_c}c_\phi + \dot{y_c}s_\phi + b\dot{\phi} \\ \dot{\theta}_l r &= \dot{x_c}c_\phi + \dot{y_c}s_\phi - b\dot{\phi} \\ 0 &= \dot{y_c}c_\phi - \dot{x_c}s_\phi - d\dot{\phi} \end{aligned}\right\} \quad (1)$$

Relaxing the pure rolling assumption and letting the wheels slip in both directions, the relationship between linear velocities of the right and left wheels $(\dot{\rho_r}, \dot{\rho_l})$ and the lateral velocity of the wheel $(\dot{\eta})$ to the velocity of the center of mass of the robot can be written as,

$$\left.\begin{aligned} \dot{\rho_r} &= \dot{x_c}c_\phi + \dot{y_c}s_\phi + b\dot{\phi} \\ \dot{\rho_l} &= \dot{x_c}c_\phi + \dot{y_c}s_\phi - b\dot{\phi} \\ \dot{\eta} &= \dot{y_c}c_\phi - \dot{x_c}s_\phi - d\dot{\phi} \end{aligned}\right\} \quad (2)$$

The presence of slip requires additional variables in the form of the longitudinal velocities of the two wheels and the lateral velocity. Considering these additional variables the generalized position vector describing the robot motion is $q = [x_c, y_c, \phi, \rho_r, \rho_l, \eta, \theta_r, \theta_l]^T$. Let m_t be the total mass of the robot, m_w be the mass of the wheel, F_{long} be the longitudinal traction force, F_{lat} be the lateral traction force, r be the radius of the wheel, I_t be the total moment of inertia of the robot in the plane of robot movement, I_{wy} be the moment of inertia of the wheel in the plane of rotation, $m_{13} = 2dm_w s_\phi$, $m_{23} = 2dm_w c_\phi$, $O_{n\times n}$ and $I_{n\times n}$ be the null and identity matrices, respectively. Define

$$\begin{aligned} B(q) &= [O_{6\times 2}, I_{2\times 2}]^T,\ T = [\tau_r, \tau_l]^T \\ f_{11} &= (F_{longr} + F_{longl})c_\phi - (F_{latr} + F_{latl})s_\phi \\ f_{21} &= (F_{longr} + F_{longl})s_\phi + (F_{latr} + F_{latl})c_\phi \\ f_{31} &= (F_{longr} - F_{longl})b - (F_{latr} + F_{latl})d \end{aligned} \quad (3)$$

$$C(q,\dot{q}) = \begin{bmatrix} 2dm_w\dot{\phi}^2 c_\phi \\ 2dm_w\dot{\phi}^2 s_\phi \\ 0 \\ -\dot{\phi}(\dot{x_c}c_\phi + \dot{y_c}s_\phi) \\ -\dot{\phi}(\dot{x_c}s_\phi - \dot{y_c}c_\phi) \\ -\dot{\phi}(\dot{x_c}s_\phi - \dot{y_c}c_\phi) \\ 0 \\ 0 \end{bmatrix} \quad F(q) = \begin{bmatrix} f11 \\ f21 \\ f31 \\ 0 \\ 0 \\ 0 \\ -rF_{longr} \\ -rF_{longl} \end{bmatrix}$$

$$M(q) = \begin{bmatrix} M_1 & O_{3\times 3} & O_{3\times 2} \\ M_2 & -I_{3\times 3} & O_{3\times 2} \\ O_{2\times 3_{13}} & O_{2\times 3} & I_{wy}I_{2\times 2} \end{bmatrix}$$

$$M_1 = \begin{bmatrix} m_t & 0 & m_{13} \\ 0 & m_t & -m_{23} \\ m_{13} & -m_{23} & I_t \end{bmatrix} \quad M_2 = \begin{bmatrix} -s_\phi & c_\phi & -d \\ c_\phi & s_\phi & b \\ c_\phi & s_\phi & -b \end{bmatrix}$$

The dynamics of the robot under slip are given by,

$$M(q)\ddot{q} + C(q,\dot{q}) = B(q)T + F(q) \tag{4}$$

To calculate the normal forces, consider the Figures 2 and 3 showing the front and lateral views of the robot, respectively, and the various forces involved. We assume the robot is constructed such that its mass is uniformly distributed along the longitudinal axis. Therefore, the center of mass lies on the longitudinal axis, and its distance to the center of the caster wheel is defined as e. We assume that the point at which the caster wheel makes contact with the ground surface when projected onto the robot platform plane falls on the longitudinal axis. One can find relationships of normal forces with the other forces involved from Figures 2 and 3. Let N be the normal force, g be the acceleration due to gravity, h be the height of the center of mass of robot from the ground, and the subscript ca denote the caster wheel. These relationships are given by

$$N_r + N_l + N_{ca} = m_t g \tag{5}$$

$$(F_{latr} + F_{latl})h + N_l b = N_r b \tag{6}$$

$$N_{ca}(d+e) = m_t g d \tag{7}$$

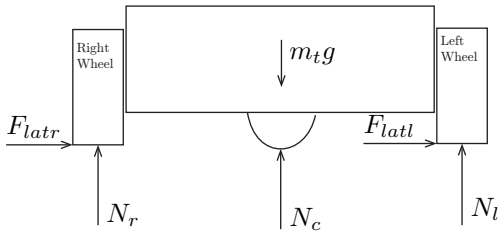

Fig. 2: Front view of the robot showing various forces

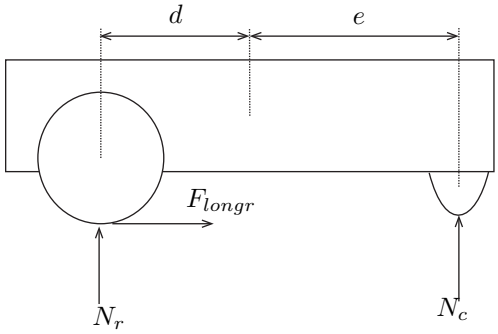

to

Fig. 3: Lateral view of the robot showing various forces

If we consider two caster wheels positioned in the front of the robot as shown in Figure 4, with the above analysis the force and moment balance equations can be written as

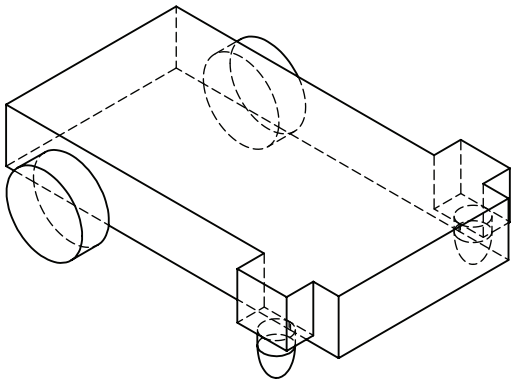

Fig. 4: Scheme of a robot with two caster wheels

$$N_r + N_l + N_{car} + N_{cal} = m_t g \tag{8}$$

$$(F_{latr} + F_{latl})h + (N_l + N_{cal})b = (N_r + N_{car})b \tag{9}$$

$$(N_{car} + N_{cal})(d+e) = m_t g d \tag{10}$$

Notice that this method can be extended for more caster wheels.

III. Wheel Traction Forces

It is necessary to determine the traction forces to solve the dynamics of the robot under slip conditions. Consider a wheel that is rotating under pure rolling condition. Then the total force on the wheel can be expressed in terms of applied torque (τ) as,

$$F = m_w a = m_w \ddot{\theta} r = m_w \left(\frac{\tau - Fr}{I_{wy}}\right) r$$

$$\implies F = \frac{\tau m_w r}{m_w r^2 + I_{wy}} \tag{11}$$

For the entire robot we have

$$F = \frac{\tau \frac{m_t}{2} r}{\frac{m_t}{2} r^2 + I_{wy}} = \frac{\tau m_t r}{2I_{wy} + m_t r^2} \tag{12}$$

Using the Coulomb friction model to determine the value of the maximum force that has to be applied on the wheel before it starts to slip, we obtain

$$F_{max} = \mu_s N \tag{13}$$

where μ_s is the static friction coefficient. The wheel slips if the value of F in Equation (11) is greater than Equation (13). Once the wheel starts to slip the amount

of force that is spent on the linear motion of the wheel is given by

$$F_{lin} = \mu_k N \tag{14}$$

where μ_k is the kinetic friction coefficient. Thus the difference between the applied force (Equation (11)) and the force given by Equation (14) causes the wheel to continue slipping. Lateral slip of the wheel may occur in conjunction with longitudinal slip. When the wheel is slipping, decomposing the total linear force due to the applied torque into lateral and longitudinal force components as shown in Figure 5 we obtain

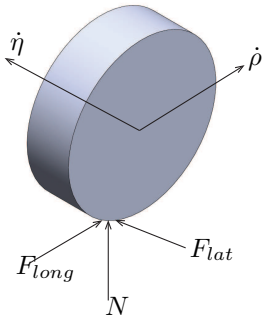

Fig. 5: Longitudinal and lateral slip due to friction forces

$$F_{longr} = \mu_k N_r \left(\frac{\dot{\rho_r}}{\sqrt{\dot{\rho_r}^2 + \dot{\eta}^2}}\right) \tag{15}$$

and

$$F_{latr} = \mu_k N_r \left(\frac{\dot{\eta}}{\sqrt{\dot{\rho_r}^2 + \dot{\eta}^2}}\right) \tag{16}$$

These components are used to compute the accelerations in the respective directions which are then used to calculate the displacement. Similar force components can be obtained for left wheel. One should notice that the normal forces play an important role in the determination of the traction forces, and the value of the normal forces in-turn depends on the position of the caster wheel(s).

A. Slip avoidance control strategy

The wheel slip is determined by the traction forces acting on it. Hence using the traction forces if we limit the applied torques on the wheels such that the reaction force is less than the maximum allowable force F_{max}, slip can be avoided. Thus mathematically the maximum torque that can be applied to the wheel to ensure that there is no slip is obtained by equating Equation (12) to the value $\mu_s N$ as

$$\tau_{max} = \frac{\mu_s N(2I_{wy} + m_t r^2)}{m_t r} \tag{17}$$

The normal force N in the above equation is either N_r or N_l depending on the wheel in consideration.

IV. Model Simulations and Experiments

Numerical simulations are conducted for a range of input torques using the parameters from an actual robot shown in Figure 6 and the surface on which it is tested. The

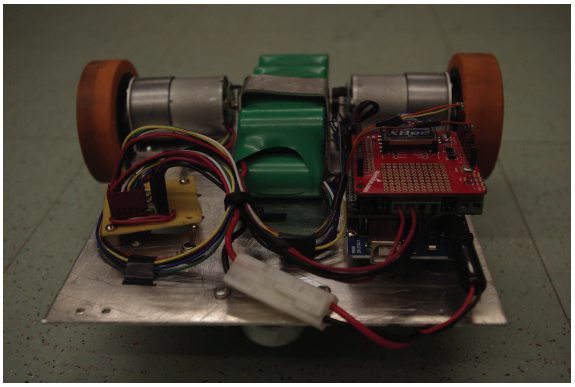

Fig. 6: Mobile robot used in experiments

values used are $\mu_s \approx \mu_k$ = 0.241, $2b$ = 0.21 m, e = 0.095 m, d = 0.055 m, g = 9.81 m/s, h = 0.0216 m, m_r = 1.5 kg, I_{rz} = 0.009753 kg m^2, I_{wz} = 0.000584 kg m^2, I_{wy} = 0.001168 kg m^2, r = 0.0365 m, m_w = 0.064 kg. Using these numerical values in Equation (17) the maximum allowable torque is 0.095 m-N. Note that the values of the coefficients of friction μ_s and μ_k were obtained through experiments for the wheel and surface used.

A torque input based on a velocity profile for a straight line trajectory is used for simulations and experiments. The robot is accelerated for 0.5 seconds using a constant input torque, after which the torque is set to zero. The torque values that are used in these tests are, (a) torque value below the maximum allowable torque limit (0.09 m-N), (b) torque value above this limit (0.1 m-N), and (c) maximum rated torque of the motors (0.13 m-N). The wheel angular velocity and the position of the robot obtained from simulations are shown in Figures 7 and 8, respectively. Observe that the angular velocity of the wheel increases in proportion to the torque but the final positions of the robots do not change significantly. This is due to the fact that once the wheel starts slipping only a portion of the input torque is used in moving the

wheel forward. The amount of the input torque used in moving the wheel is determined by the kinetic friction coefficient and remains unchanged.

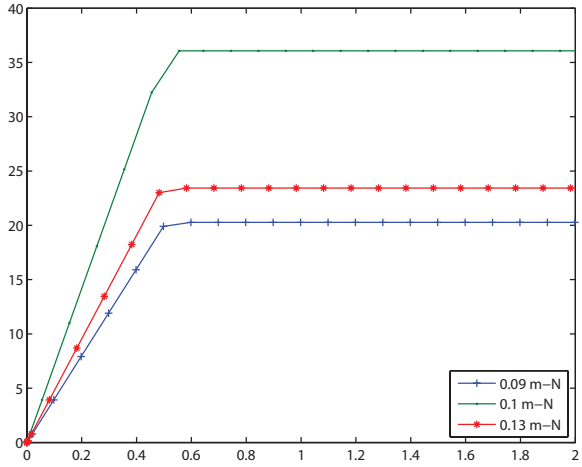

Fig. 7: Evolution of wheel angular velocity (rad/s) for torques: 0.09 m-N, 0.1 m-N, and 0.13 m-N

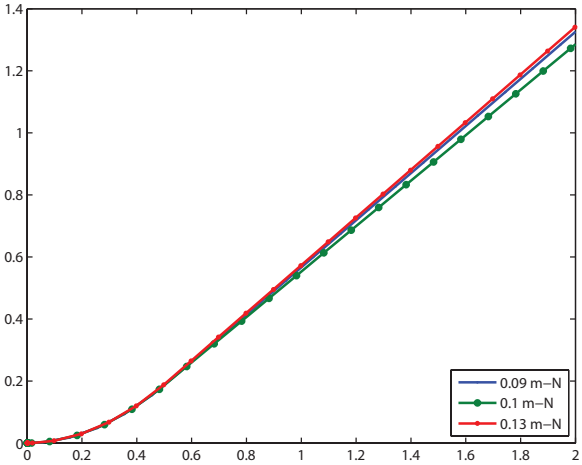

Fig. 8: Evolution of robot position (meters) for different torques and accelerations: 0.09 m-N and 44 rad/s^2, 0.1 m-N and 48 rad/s^2, and 0.13 m-N and 72 rad/s^2

Experiments are conducted to verify the model simulation results shown above, and the torque limiting control strategy. Encoders on wheels are used to measure wheel angular position and velocity. The actual robot position is determined using a video camera on the ceiling above the robot. The same torque profiles used in model simulations are also used in the experiments.

The following three reference acceleration values were employed: 44, 48, and 72 rad/s^2. Figure 9 shows the evolution of the wheel angular velocity with the three torque profiles along with the angular velocity obtained using the torque limiting control strategy for the case of 72 rad/s^2. It should be noted that the average value of the angular velocities are comparable to the ones obtained using model simulations. Also notice that the angular velocity in the experiment with the control strategy is close to the non-slip condition i.e, 44 rad/s^2. Position measurements obtained from the encoder and the video are shown in Figure 10 for 44 and 48 rad/s^2. For 48 rad/s^2 the robot position measured by the camera is less than that from the encoders which implies the wheels are slipping and the encoders failed to measure the true position of the robot. Comparing the position and angular velocities for the 44 and 48 rad/s^2 cases the torque limit calculated in the previous section is verified. Figure 11 shows the position when torque limiting control is applied, where the wheel acceleration is successfully limited to avoid slip.

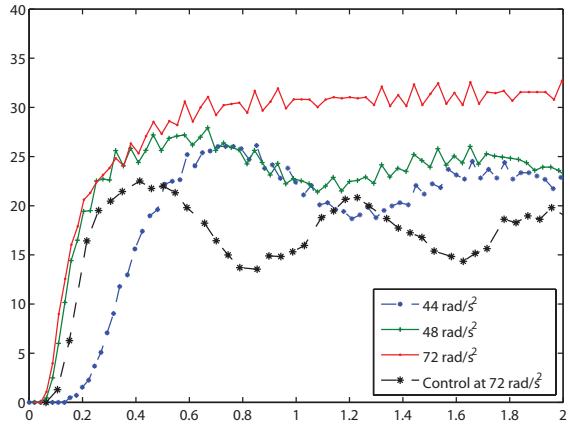

Fig. 9: Measured angular velocity of the wheel (rad/s)versus time at: 44 rad/s^2, 48 rad/s^2, 72 rad/s^2, and at 72 rad/s^2 with torque control

V. Conclusions

A traction force model is developed by considering a simple Coulomb friction model. The linear velocities of the wheel are used in computing these traction forces. The dynamic analysis shows that the caster wheel plays an important part in determining the traction forces. Simulations of the differential drive dynamics using the proposed traction model reveal the occurrence of slip if the applied torque is greater than the maximum allowed torque which depends on the coefficient of static friction. Experimental results are comparable to model simulation results in terms of the wheel angular

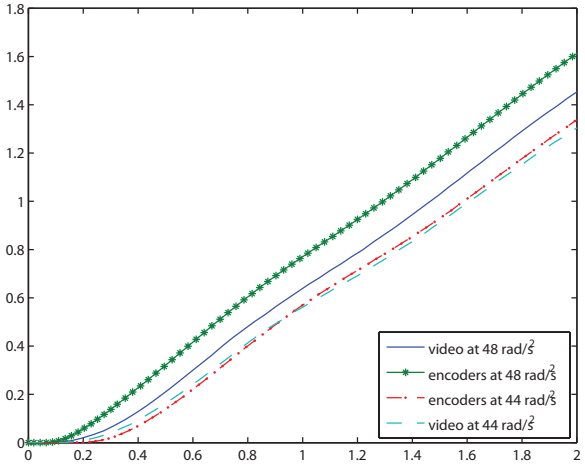

Fig. 10: Measured Robot position versus time at: 44 rad/s^2 and 48 rad/s^2 with encoders and video

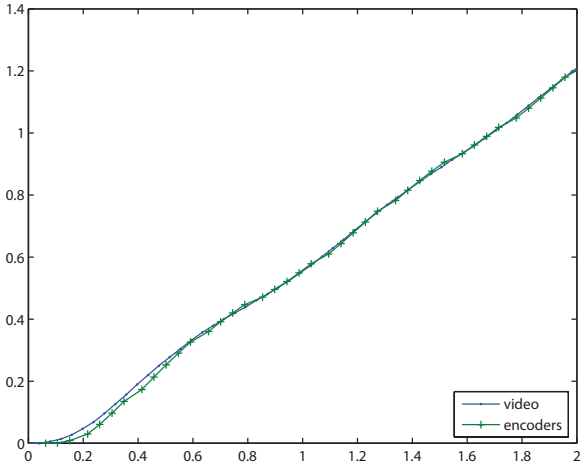

Fig. 11: Evolution of the measured Robot position at 72 rad/s^2 with torque control

velocities and robot position. Thus verifying the torque limit between slip and no-slip conditions. Future work will involve the development of a model based nonlinear controller that is applicable to motion under both slip and no slip conditions. A simple friction model based on the coefficient of static friction is used to obtain the limiting torque value that is employed to distinguish between slip and no slip conditions. Future work will consider the use of a nonlinear friction model that depends on wheel velocities.

REFERENCES

[1] Y. Kanayama, Y. Kimura, F. Miyazaki, and T. Noguchi, "A stable tracking control method for an autonomous mobile robot," in *Proceedings of IEEE International Conference on Robotics and Automation*, pp. 384–389 vol.1, 1990.

[2] X. Yun and Y. Yamamoto, "Internal dynamics of a wheeled mobile robot," in *Proceedings of IEEE/RSJ International Conference on Intelligent Robots and Systems*, vol. 2, pp. 1288–1294 vol.2, 1993.

[3] Y. Zou, *Distributed Control of Multiple Vehicle Systems using Constraint Forces*. PhD thesis, Oklahoma State University, Stillwater, OK, USA, 2008.

[4] A. Gholipour and M. Yazdanpanah, "Dynamic tracking control of nonholonomic mobile robot with model reference adaptation for uncertain parameters," in *Proc. of the European Control Conference*, 2003.

[5] A. Albagul, Wahyudi, and Wahyudi, "Dynamic modeling and adaptive traction control for mobile robots," in *Proceedings of 30th Annual Conference of IEEE Industrial Electronics Society*, vol. 1, pp. 614–620 Vol. 1, 2004.

[6] S. Konduri, "Coordination of multiple autonomous vehicles with directed communication graphs," Master's thesis, Oklahoma State University, 2012.

[7] L. Li, F.-Y. Wang, and Q. Zhou, "Integrated longitudinal and lateral tire/road friction modeling and monitoring for vehicle motion control," *IEEE Transactions on Intelligent Transportation Systems*, vol. 7, no. 1, pp. 1–19, 2006.

[8] R. Balakrishna and A. Ghosal, "Modeling of slip for wheeled mobile robots," *IEEE Transactions on Robotics and Automation*, vol. 11, no. 1, pp. 126–132, 1995.

[9] S. Shekhar, "Wheel rolling constraints and slip in mobile robots," in *Proceedings of IEEE International Conference on Robotics and Automation*, vol. 3, pp. 2601–2607 vol.3, 1997.

[10] K. Yoshida and G. Ishigami, "Steering characteristics of a rigid wheel for exploration on loose soil," in *Proceedings of IEEE/RSJ International Conference on Intelligent Robots and Systems*, vol. 4, pp. 3995–4000 vol.4, 2004.

[11] P. Lamon, A. Krebs, M. Lauria, R. Siegwart, and S. Shooter, "Wheel torque control for a rough terrain rover," in *Proceedings of 2004 IEEE International Conference on Robotics and Automation*, vol. 5, pp. 4682–4687, IEEE, 2004.

[12] J.-S. Young and B.-J. Wu, "The analysis of the dynamics for the unturned wheels of vehicles," in *The International Conference on Electrical Engineering*, 2008.

[13] S. N. Sidek and N. Sarkar, "Dynamic modeling and control of nonholonomic mobile robot with lateral slip," in *Third International Conference on Systems*, pp. 35–40, 2008.

[14] Y. Tian, N. Sidek, and N. Sarkar, "Modeling and control of a nonholonomic wheeled mobile robot with wheel slip dynamics," in *IEEE Symposium on Computational Intelligence in Control and Automation*, pp. 7–14, 2009.

[15] S. Nandy, S. Shome, R. Somani, T. Tanmay, G. Chakraborty, and C. Kumar, "Detailed slip dynamics for nonholonomic mobile robotic system," in *International Conference on Mechatronics and Automation*, pp. 519–524, 2011.